Pergamon

Bioorganic & Medicinal Chemistry Letters 12 (2002) 1637–1641

BIOORGANIC & MEDICINAL CHEMISTRY LETTERS

Preparation, Characterization, Molecular Modeling and In Vitro Activity of Paclitaxel–Cyclodextrin Complexes

Stefano Alcaro,[a] Cinzia Anna Ventura,[b] Donatella Paolino,[c] Danilo Battaglia,[a] Francesco Ortuso,[a] Luigi Cattel,[d] Giovanni Puglisi[c] and Massimo Fresta[a,*]

[a]*Department of Pharmacobiological Sciences, University 'Magna Græcia' of Catanzaro, Complesso 'Ninì Barbieri', I-88021 Roccelletta di Borgia (CZ), Italy*

[b]*Pharmaco-Chemical Department, University of Messina, Viale Annunziata, I-98168 Messina, Italy*

[c]*Department of Pharmaceutical Sciences, University of Catania, Viale Andrea Doria n. 6, I-95125 Catania, Italy*

[d]*Department of Drug Science and Technology, University of Torino, Via P. Giucia 9, I-10125 Turin, Italy*

Received 3 January 2002; revised 14 March 2002; accepted 3 April 2002

Abstract—Paclitaxel (**PTX**) was complexed with β-cyclodextrin (**1**), 2,6-dimethyl-β-cyclodextrin (**2**) and 2,3,6-trimethyl-β-cyclodextrin (**3**). **PTX**–CYD complexes were characterized both at the solid and liquid states. Experimental findings are in agreement with molecular modeling analysis, which showed different **PTX**–CYD interaction as a function of macrocyle methylation. The complexation of **PTX** within the CYD cavity preserved its antitumoral activity. © 2002 Published by Elsevier Science Ltd.

Paclitaxel (**PTX**) is an anticancer agent used in breast, ovarian, lung, head and neck cancers.[1] Its mechanism of action is based on the interaction with the mitotic fuses.[2] The hydrophobic chemical structure of **PTX** (Fig. 1) is characterized by very low water solubility; thus, it must be formulated as a micellar solution made up of polyoxyethylated castor oil and 50% absolute ethanol. This formulation triggers severe acute adverse effects both in animals and humans[3] and thus a prophylactic regimen is necessary to reduce the hypersensitivity reactions.[4]

Alternative dosage forms such as cyclodextrins (CYDs) can be used as **PTX** drug delivery systems.[5] CYDs, acting as hosts, are able to include apolar substances in their hydrophobic cavity, thus modifying physicochemical characteristics of the guests.[6]

In this paper, the preparation of **PTX** complexes with various CYDs was carried out. The inclusion ability of CYDs towards **PTX** was investigated as a function of the macrocycle substitutions, namely β-cyclodextrin (**1**), 2,6-dimethyl-β-cyclodextrin (**2**) and 2,3,6-trimethyl-β-cyclodextrin (**3**), were studied. Molecular modeling investigations on the **PTX**–CYD interaction were carried out with the aim of clarifying energetically and structurally the recognition process.

PTX was kindly provided by Indena (Italy) and used without further purification. The purity grade, determined by HPLC, was 97.6% (w/w). CYDs were a gift of Roquette (Cassano Spinola, Italy). All other chemicals were analytical grade reagents. Double distilled water was used throughout.

The inclusion complexes of **PTX** with CYDs were prepared by the freeze-drying method.[7] Briefly, **PTX** (10 mg) was solubilized in ethanol (12 mL) in the dark at room temperature. CYD aqueous solutions (14 mL) at various concentrations (3.5, 5, 7% w/v) were added to

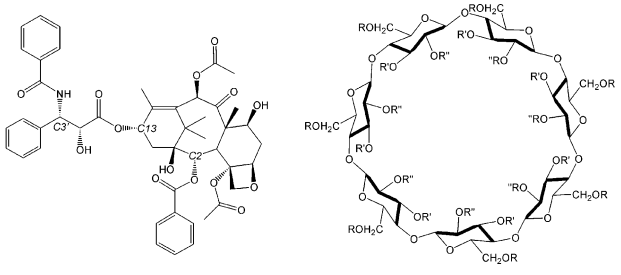

Figure 1. Chemical formulae of **PTX** (left) and cyclodextrins **1** (R = R′ = R″ = H), **2** (R′ = H, R = R″ = CH_3) and **3** (R = R′ = R″ = CH_3).

*Corresponding author. Fax: +39-0961-391490; e-mail: fresta@unicz.it

0960-894X/02/$ - see front matter © 2002 Published by Elsevier Science Ltd.
PII: S0960-894X(02)00217-2

the ethanol solution. Final hydroalcoholic solutions were stirred for 5 h at room temperature and then freeze-dried.

The **PTX**–CYD complexes were characterized both at the solid state (FT-IR spectroscopy and DSC) and at the liquid state [^{1}H NMR, circular dichroism (CD)]. FT-IR spectra were carried out on KBr disks using a Perkin-Elmer mod. 1600 FT-IR spectrophotometer. DSC analyses were recorded on a Mettler DSC 12E equipped with a Haake D8-G cryostat. Mettler TA89A software was used for data acquisition and analysis. The scanning rate was 10 °C/min from 30 to 300 °C under a nitrogen flow. CD spectra of free **PTX** or **PTX**/CYD mixtures in a methanol/water solution (30:70 v/v) were carried out with a Jasco J-600D recording spectropolarimeter. ^{1}H NMR spectra were measured using a Varian Unit Inova 200 MHz at a probe temperature of 303 K. Samples were dissolved in a water/methanol (70/30 v/v) solution. In all cases, the residual signal of HDO at 4.83 ppm was used as reference.[8]

The increase of **PTX** water solubility in the presence of the various CYDs was evaluated using the Higuchi and Connors method.[9] Samples were filtered and then analyzed by HPLC (1050 Hewlett Packard apparatus) to determine the drug concentration. An apparent 1:1 stability constant (K_c) of **PTX**–CYD systems was calculated from the straight portion of the phase solubility diagrams.[9]

The molecular modeling study was carried out using a three-step approach. The first one was the Monte Carlo (MC) conformational analysis of **PTX** using the MacroModel package.[10] We have considered several force fields as implemented in the software package and selected the MM3* as the most suitable for the molecular modeling of **PXT** and CYDs.[11] Based on the computational philosophy of the 'quasi-flexible' docking approach of the in-house software MOLINE,[12] we then carried out the second step adopting three 'open' conformations that were equal for all the CYDs,[13] and the forty most **PXT** stable conformers found in the MC search within 5 kcal/mol above the global minimum. This approach ensures an unbiased computational treatment of the three different CYDs allowing a simple, direct comparison of the docking results. In the third step, the minimum energy complexes within 3 kcal/mol were submitted to the full energy refinement using different force fields both in vacuo and in GB/SA water.[14] In this step, the complex conformations are free to relax, generating the induced fit effects. The energetic–thermodynamic comparison with the experimental results was implemented as the criterion for the identification of the most appropriate computational protocol to adopt for the structural characterization of the **PTX**–CYD complexes. Such advanced analysis was carried out by geometrical descriptors able to indicate which **PTX** moiety is able to give inclusion into the CYD cavity and from which side.

The antitumoral effectiveness of **PTX**–CYD complexes were assayed in vitro with respect to the free drug. DU 145 (human hormone-resistant prostate cancer) cells were used, and cell lines were cultured in DMEM, 10% fetal calf serum, 0.1% antibiotics (penicillin, streptomycin) at 37 °C in a 5% CO_2 humidified atmosphere. Cells were seeded in 24-well plates (1×10^5 cells per mL per well) and the compounds were added. After 72 h incubation, cells were counted with a haemocytometer by the trypan blue exclusion assay.[15]

The freeze-drying preparation procedure led to the formation of amorphous samples that were investigated to evaluate the formation of **PTX**–CYD complexes. FT-IR analysis showed that the intensity of the **PTX** carbonyl-ester stretching band at 1730 cm^{-1} was significantly reduced in the case of CYD complexation. A broadening of the 1600–1650 cm^{-1} carbonyl stretching was also observed. The crystal structure of **PTX** is characterized by a network of hydrogen bonding involving the carbonyl ester, the 2′-OH and the 3′-NH of the side chain.[16] These IR spectra changes could be evidence of the hydrogen bond alteration[5] as a consequence of the drug interaction with CYDs.

Solid state characterization by DSC showed the disappearance of the drug fusion peak at 222 °C in the case of **PTX**–CYD complexes, whereas this endothermic peak was still present in **PTX**–CYD physical mixtures. These findings were considered evidence of an interaction at the solid state between **PTX** and CYDs.[17] Exothermic peaks observed in the DSC scans of the **PTX**–CYD solid samples could be attributed to a heat-induced transition from the amorphous to the crystalline state.[18]

The interaction of **PTX** with CYDs was also studied in an aqueous solution by evaluating the influence of various macrocycles on spectroscopic characteristics of the drug. In particular, **PTX** shows two CD bands (Fig. 2): at 230 nm (positive) and at 290 nm (negative).

An increase of the intensity of both bands was observed in the presence of different concentrations of **2**, particularly at 1:100 and 1:1000 mole ratios. A shift of 1–2 nm towards lower wavelengths was observed for both bands. The intensity increase of the negative band was due to the variation of the aromatic group environment

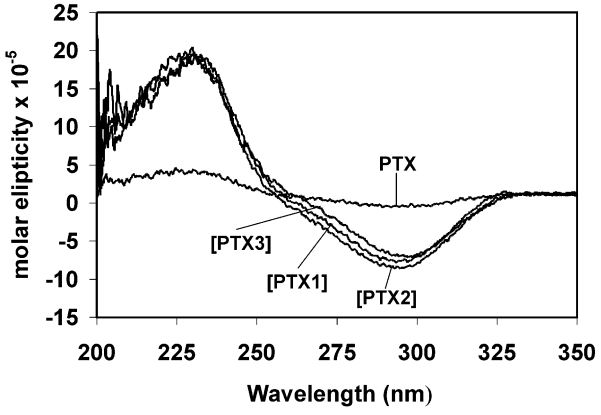

Figure 2. CD spectra of free TAX or in the presence of different CYDs in a 1:100 drug/CYD molar ratio.

as a consequence of **PTX** complexation into the CYD cavity, while the effect on the positive band could demonstrate the **PTX** desaggregation into monomers.[5] Other CYDs influence the CD bands of the drug to a lesser extent compared to **2** (Fig. 2). Taking into account the magnitude of the intensity variation triggered by various CYDs, **2** seemed to have the highest affinity for **PTX**.

^{1}H NMR experiments gave no information about **PTX** complexation into the CYD cavity, that is no shift was observed for **PTX** or CYD signals. The absence of NMR signals could be due to a rapid turnover of the **PTX**–CYD complex with respect to the μs NMR temporal resolution.[5]

As concerns solubility studies at 25 °C, an increase of water solubility was observed in the presence of all CYDs. In particular, **1** showed a Bs type isotherm (due to the limited solubility of this complex), while A_L type isotherms were obtained for the other CYDs.[9] The **PTX** solubility increase was strictly related to the magnitude of the interaction of the drug with CYDs, thus confirming the higher affinity of **PTX** for the apolar cavity of **2** with respect to other CYDs. As regards **3**, the 3′-OCH_3 increased the apolar characteristic of the cavity, but it produced a steric hindrance for the **PTX** complexation as demonstrated theoretically by our computational studies. In all cases the complexes were weak, being characterized by low stability constants (K_c) (Table 1). In fact, the bulky structure of **PTX** can not entirely penetrate into CYD cavities, and the complexation is limited to the aromatic ring present on the sidechain and/or the 2-benzoyl group of the taxane ring.[5]

Table 1. Stability constants for the **PTX**–CYD complexes in water

Complex	K_c (M^{-1})		
	25±0.5 °C	37±0.5 °C	45±0.5 °C
[PTX·1]	337	196	63
[PTX·2]	406	310	270
[PTX·3]	355	222	103

Table 2. Complexation enthalpies[18] of **PTX**–CYD complexes in vacuo and GB/SA water computed with the MM3* force field at 300 K

Complex	·H in vacuo	Δ*H* in GB/SA water
[PTX·1]	−28.96	−22.04
[PTX·2]	−30.64	−24.42
[PTX·3]	−19.88	−22.82

The computational protocol best fitting the experimental stability constant trend was evaluated based on the correlation with the computed complexation enthalpy differences.[19] The MM3* force field was able to reproduce the experimental trend (Table 2). The best correlation was found taking into account the solvation effect, which plays a relevant role in the stability of the three inclusion complexes.

Data in Table 2 show the relevance of the solvation effect for the CYDs **1** and **2**, which have some free hydroxyl groups able to donate hydrogen bonds to the solvent. In **[PTX·1]** and **[PTX·2]** complexes, the solvation penalty was remarkable: ∼7 and ∼6 kcal/mol, respectively. On the other hand, **3** is unable to act as hydrogen bond donator and its complex in water is moderately favored (approx. −3 kcal/mol).

In order to make a characterization of the recognition process at the molecular level, dummy atoms (DA), representative of ring or macrocycle centroids, were extensively used for the calculation of significant geometrical descriptors. The three aromatic rings of the **PTX** that, presumably, can give inclusion interaction within the cavity of the CYDs, were considered. In particular two concomitant informations have been taken into account: the complexation of each phenyl ring into the cavity[20] and the direction of the inclusion.[21] In Table 3, the percentage estimation is reported considering the Boltzmann probability at room temperature of the complex microstates satisfying both distance and direction criteria.

A detailed analysis of the most populated complex conformers in GB/SA water is reported in Table 4.

Data in Tables 3 and 4 demonstrate the ability of CYDs to make inclusion complexes mainly in the *large* cavity. Only **1** in GB/SA water seems to prefer the *small* one. The explanation of such behavior is related to the hydrogen bond interactions of **1** with the solvent. In this case, energetically favored by the secondary hydroxyl groups that are free to interact with the bulky water, the drug inclusion occurs through the *small* cavity.

Table 3. Geometrical descriptors, expressed as average Boltzmann probability percentage at 300 K, computed onto the MM3* complex ensembles in vacuo[a] and GB/SA water[b]; the *large* and *small* recognition patterns refer to the cavity entrance direction of the inclusion[21]

PTX	**[PTX·1]**		**[PTX·2]**		**[PTX·3]**	
Aromatic ring	Large	Small	Large	Small	Large	Small
Phenyl in 3′ sidechain	68.5[a]	0.4[a]	94.2[a]	0.0[a]	17.6[a]	0.0[a]
	0.0[b]	84.2[b]	96.8[b]	0.1[b]	38.8[b]	0.0[b]
Benzamide in 3′ sidechain	18.1[a]	0.0[a]	0.0[a]	0.0[a]	0.0[a]	0.0[a]
	0.0[b]	13.6[b]	0.0[b]	0.0[b]	0.2[b]	0.0[b]
Benzoate in 2 macrocycle	12.8[a]	0.0[a]	0.7[a]	0.0[a]	56.1[a]	0.0[a]
	0.0[b]	0.0[b]	3.1[b]	0.0[b]	50.0[b]	0.0[b]

As concerns the inclusion preference, the phenyl group in the 3′ position is the preferred one. The most populated complex conformers in GB/SA water are characterized by the stabilization effect of one intermolecular hydrogen bond between the acetate in 10 onto the **PTX** macrocycle and one primary hydroxyl of **1** (Table 4).

2 has a high degree of **PTX** inclusion through the *large* rim in all conditions. The primary hydroxyl methylation drastically prevents the inclusion through the *small* cavity rim. The preferred phenyl for the inclusion is again that in the 3′ position but, in this case, an almost exclusive preference close to 100% was observed, showing how the partial methylation of the secondary hydroxyl groups dramatically influences the recognition of such an aromatic ring. This data is consistent with the energy stabilization of the [**PTX·2**] complex with respect to the [**PTX·1**] and [**PTX·3**] ones as shown in Tables 1 and 2. Also in this case, one intermolecular hydrogen bond was observed, but between the **PTX** hydroxyl group in 2′ and one free secondary hydroxyl group of **2** (Table 4). In Fig. 3, the global minimum energy conformation of such a complex is shown.

2 and **3** show an incompatibility to give inclusion through the *small* cavity rim. Also the *large* one possess a certain difficulty in the inclusion property as revealed by the sum of the three phenyl probabilities in vacuo as well as in GB/SA water. In both cases no saturation was observed, suggesting that several populated associations occur without inclusion. In the case of **3**, the most favored phenyl ring for the inclusion is the benzoate moiety in the 2 position of the **PTX**. This feature can be explained as a consequence of the steric hindrance due to the full methylation of the secondary hydroxyl group of **3**. In such condition, the drug cannot fit easily through the *large* cavity rim with the 3′ phenyl, sterically less accessible due to the presence of the close bulky benzamide group. The full methylation also prevented the hydrogen donor contribution to the drug that could stabilize the bimolecular complex. As shown in Table 4, only **3** complexes have no hydrogen bond stabilization.

The biological effectiveness of free or complexed PTX was evaluated against DU 145 tumoral cells (Table 5). **2** and **3** showed a certain toxicity against tumoral cells. This finding can be correlated to the capacity of these two CYDs to influence the cellular membrane permeability and packing order.[22] Various complexes showed different antitumoral activity with respect to free **PTX**. In particular, **[PTX·1]** showed a greater antitumoral activity than the free drug at high dilution factors. On the contrary, other complexes showed a reduction of this activity. These data can be due to three different factors: (i) the higher the complex K_c values the lower the availability of the drug to the permeation through the cellular membrane, (ii) the higher the complex solubility the greater the amount of drug reaching the

Table 4. Detailed analysis of most populated complex conformers in MM3* GB/SA water ensembles

Conf	[PTX·1]			[PTX·2]			[PTX·3]		
	P%[a]	HB[b]	Ph/ver[c]	P%[a]	HB[b]	Ph/ver[c]	P%[a]	HB[b]	Ph/ver[c]
1	18.79	1	3′/S	28.84	1	3′/L	35.24	0	3′/L
2	18.05	1	3′/S	27.71	1	3′/L	27.7	0	2/L
3	16.00	1	3′/S	24.57	1	3′/L	9.77	0	2/L
4	13.63	1	3′/S	6.29	1	3′/L	6.28	0	2/L

[a]Boltzmann population at room temperature.
[b]Number of intermolecular hydrogen bonds between **PTX** and CYDs.
[c]PXT phenyl ring position complexed into the cavity and the inclusion versus L (large) or S (small).

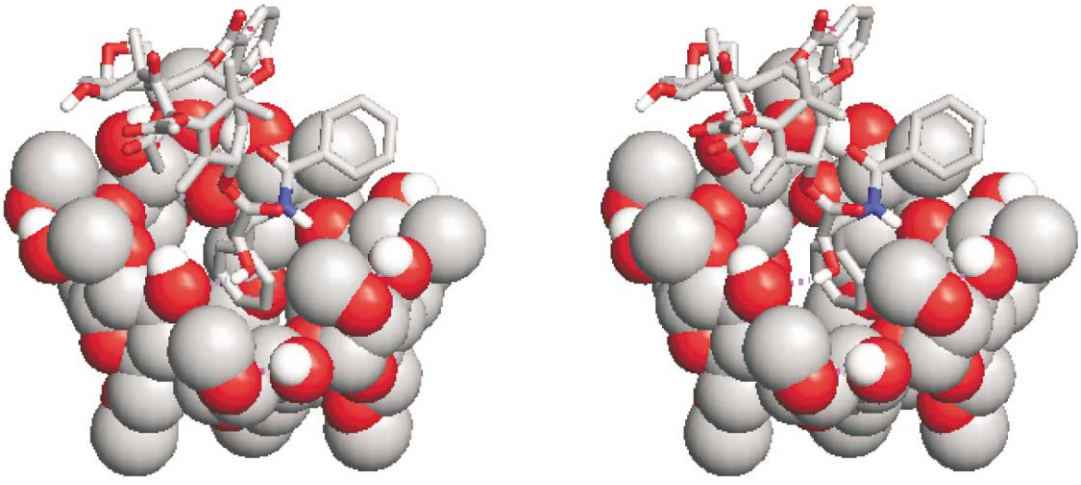

Figure 3. Stereoview representation of the [**PTX·2**] global minimum conformer obtained with MM3* in GB/SA water. The **PTX** and the CYD **2** are respectively shown in polytube and CPK representation. The violet dashed lines highlight the hydrogen bond network.

Table 5. In vitro activity of free PTX or complexed within **1**,**2** or **3** against DU 145 cells; results are expressed as percentage of cellular survival as a function of drug dilution[a]

Sample	**PTX** dilution factor			
	1:50	1:100	1:500	1:1000
PTX[b]	11.6±0.2	12.1±0.4	43.3±1.6	46.0±1.8
1	96.4±1.7	96.6±1.4	96.4±1.3	96.8±2.1
[PTX·1]	12.2±2.1	22.3±2.3	23.1±1.9	24.2±2.6
2	88.9±0.4	90.6±0.9	90.2±0.5	91.5±0.3
[PTX·2]	35.2±0.9	46.3±2.1	51.1±1.9	61.3±2.4
3	79.7±0.5	85.5±0.8	87.0±0.4	90.1±0.7
[PTX·3]	43.2±0.8	61.3±1.3	68.7±1.5	69.3±1.9

[a]Controls (untreated cells) showed a 100% survival.
[b]PTX was solubilized in DMSO, which showed a certain toxicity against DU 145 cells.

surface of tumoral cells, (iii) the higher the penetration enhancer effect of CYD the greater the amount of drug that is able to permeate through the cellular membrane.[23] Therefore, **1** is able to increase the drug solubility in a similar way to **2** and **3**, it can allow the transfer of the drug from the CYD cavity to tumoral cells (lower K_c than **2**) and it can exert a cellular membrane permeation enhancer effect.[22]

In conclusion, the progressive methylation of the CYD hydroxyl groups modulates the molecular recognition towards the antitumor compound. [**PTX·2**] is the most stable complex, as shown experimentally and theoretically. The modeling results reveal the fundamental role of the solvent in the inclusion process.

In vitro findings show a modulation of the antitumoral activity as a function of the complex, that is an increase of the effect for [**PTX·1**] and a reduction in the case of [**PTX·2**] and [**PTX·3**]. Interestingly, the activity of the complexes seems to be correlated to some experimental and theoretical parameters. The increased solubility of **PTX** due to CYD complexation may be of particular importance in the future therapeutic applications of this anticancer agent.

Acknowledgements

The authors wish to thank the Istituto CNR di Biotecnologie Applicate alla Farmacologia for their computational support and the Scientific and Technological Research P.O.P. (Calabria 1994–1999) and COFIN 2000 for funding this research project. The authors are very grateful to Dr. Antony Bridgewood for his revision of the language of this paper.

References and Notes

1. Rowinsky, E. K.; Cazenave, L. A.; Donehower, R. C. *J. Natl. Cancer Inst.* **1990**, *82*, 1247.
2. Löwe, J.; Li, H.; Downing, K. H.; Nogales, E. *J. Mol. Biol.* **2001**, *313*, 1045.
3. Lorenz, W.; Rieman, H. J.; Schmal, A.; Schult, H.; Lang, S.; Ohmann, C.; Weber, D.; Kapp, B.; Luben, L.; Doenicke, A. *Agents Actions* **1977**, *7*, 63.
4. Weiss, R. B.; Donehower, R. C.; Wiernik, P. H.; Ohnuma, T.; Gralla, R. J.; Trump, D. L.; Baker, J. R.; VanEcho, D. A.; VonHoff, D. D.; Leyland-Jones, B. *J. Clin. Oncol.* **1990**, *8*, 1263.
5. Sharma, U. S.; Balasubramanian, S. V.; Straubinger, R. M. *J. Pharm. Sci.* **1995**, *84*, 1223.
6. Ventura, C. A.; Tirendi, S.; Puglisi, G.; Bousquet, E.; Panza, L. *Int. J. Pharm.* **1997**, *149*, 1.
7. Puglisi, G.; Ventura, C. A.; Fresta, M.; Vandelli, M. A.; Cavallaro, G.; Zappalà, M. *J. Incl. Phenom.* **1996**, *24*, 193.
8. Salvatierra, D.; Jaime, C.; Virgili, A.; Sanchez-Ferrando, F. *J. Org. Chem.* **1996**, *61*, 9578.
9. Higuchi, T.; Connors, K. A. *Adv. Anal. Chem. Instrum.* **1965**, *4*, 117.
10. MacroModel ver 6.0. Mohamadi, F.; Richards, N. G. J.; Guida, W. C.; Liskamp, R.; Lipton, M.; Caufield, C.; Chang, G.; Hendrickson, T.; Still, W. C. *J. Comput. Chem.* **1990**, *11*, 440.
11. The evaluation of the most appropriate force field has been carried out considering the RMS deviation and the internal energy of **PXT** conformers generated by MC simulation closest to its X-ray conformations, as reported by Mastropaolo, D.; Camerman, A.; Luo, Y.; Brayer, G. D.; Camerman, N. *Proc. Natl. Acad. Sci. U.S.A.* **1995**, *92*, 6920.
12. Alcaro, S.; Gasparrini, F.; Incani, O.; Mecucci, S.; Misiti, D.; Pierini, M.; Villani, C. *J. Comput. Chem.* **2000**, *21*, 515.
13. The 'open' conformation corresponds to a perfectly symmetric structure of the macrocycle ring with all the glycosidic bonds backbone fixed as $\psi = 120°$ and $\varphi = 116°$. The torsional bonds pertinent to the secondary hydroxyl (or methoxyl) groups were fixed equal for all residues ($\chi_2 = -37°$ and $\chi_3 = -43°$). The three conformations have been generated considering the *gauche* +, *gauche* − and *trans* rotamers of the χ_5 equal for all the residues.
14. Still, W. C.; Tempczyk, A.; Hawley, R. C.; Hendrickson, T. *J. Am. Chem. Soc.* **1990**, *112*, 6127.
15. Grosse, P. Y.; Bressolle, F.; Pinguet, F. *Eur. J. Cancer* **1998**, *34*, 168.
16. Vander Velde, D. G.; Georg, G. I.; Grunewald, G. L.; Gunn, C. W.; Mitscher, L. A. *J. Am. Chem. Soc.* **1993**, *115*, 11650.
17. Cabral-Marques, H. M.; Hadgraft, J.; Kellaway, I. W. *Int. J. Pharm.* **1990**, *63*, 259.
18. Hanawa, T.; Yonemochi, E.; Oguchi, T.; Nakai, Y.; Yamamoto, K. *J. Incl. Phenom.* **1993**, *15*, 91.
19. The complexation enthalpy differences ΔH have been computed using the probabilities at 300 K of each microstate and their interaction energies obtained as difference between the total energies of the complex and the isolated molecules extracted from the complex in the same conformation. In GB/SA water the ΔH contains also the solvation component.
20. We have considered the maximum threshold of 2.5 Å in the distance between the dummy atoms of the **PTX** aromatic phenyl and the macrocycle centered on the seven glycosidic oxygen atom.
21. The recognition patterns *large* and *small*, respectively, refer to the inclusion of each phenyl ring when the drug is closer to the large or to the small cavity rim of the cyclodextrin. Technically we have measured the distance between the **PTX** C13 atom and two dummy atoms averaging respectively the fourteen CYDs oxygen atoms in C2/C3 positions (center of the large entrance) and the seven methylene C6 carbons (center of the small entrance).
22. Puglisi, G.; Fresta, M.; Ventura, C. A. *J. Colloid Interface Sci.* **1996**, *180*, 542.
23. Ventura, C. A.; Fresta, M.; Paolino, D.; Pedotti, S.; Corsaro, A.; Puglisi, G. *J. Drug Target* **2001**, *9*, 379.